

A Comparison of System Architectures for a Mechanically Pumped Two-Phase Thermal Control System

Benjamin Furst¹, Eric Sunada², Stefano Cappucci³, Pradeep Bhandari⁴
Jet Propulsion Laboratory/California Institute of Technology, Pasadena, California, 91109

and

Takurou Daimaru⁵ and Hiroki Nagai⁶
Tohoku University, Sendai, 980-8579, Japan

The NASA Jet Propulsion Laboratory is developing a mechanically pumped two-phase fluid loop thermal control system to enable novel mission designs and greater science return. Pumped two-phase fluid loops have the potential to provide robust and effective thermal control that combine the best aspects of passive two-phase systems (heat pipes) and mechanically pumped single-phase fluid loops. The current program requirements include the development of a system with multiple 1 m² evaporators, each of which is capable of remaining spatially and temporally isothermal while accommodating heat loads of up to 500 W and local fluxes of up to 5 W/cm². The goal is to attain this using less than 5 W of power. Such a system would be able to accommodate the next generation of payload and bus electronics while using minimal resources. This paper compares two different mechanically pumped two-phase fluid loop architectures in the context of these requirements. A mixed flow and separated flow architecture are compared on a theoretical and experimental basis. Test data from sub-scale, single evaporator/single condenser, mixed flow and separated flow testbeds are presented. In addition, a model is introduced to better understand separated flow systems and some expressions for the theoretical performance limits of such systems are developed. To date, the investigation suggests that a separated flow architecture is better suited to the program requirements. Separated flow systems have the potential to accommodate an isothermalizing two-phase evaporator while using lower levels of power than would be required for a mixed flow system. In addition, it is argued that separated flow systems are more robust and amenable to analysis than mixed flow systems, since they significantly reduce the occurrence of two-phase flow by separating phases in the evaporator. Future work will include developing a full-scale testbed that includes multiple evaporators and condensers in a representative flight configuration.

¹ Thermal Technologist, Propulsion, Thermal, and Materials Engineering Section, 4800 Oak Grove Dr., Pasadena, CA 91109, Mail Stop 125-123.

² Senior Thermal Technologist, Propulsion, Thermal, and Materials Engineering Section, 4800 Oak Grove Dr., Pasadena, CA 91109, Mail Stop 125-123

³ Thermal Technologist, Propulsion, Thermal, and Materials Engineering Section, 4800 Oak Grove Dr., Pasadena, CA 91109, Mail Stop 125-123.

⁴ Principal Engineer, Propulsion, Thermal, and Materials Engineering Section, 4800 Oak Grove Dr., Pasadena, CA 91109, Mail Stop 125-123.

⁵ Research Associate, Department of Aerospace Engineering, 6-6-01, Aramaki-Aza-Aoba, Aoba-ku, Sendai 980-8579, Japan.

⁶ Professor, Department of Aerospace Engineering, 6-6-01, Aramaki-Aza-Aoba, Aoba-ku, Sendai 980-8579, Japan.

Nomenclature

SFA	=	Separated Flow Architecture
MFA	=	Mixed Flow Architecture
JPL	=	Jet Propulsion Laboratory
LHP	=	Loop Heat Pipe
NPSH	=	Net Positive Suction Head
P	=	fluid pressure
\dot{m}	=	mass flow rate
R	=	hydraulic resistance
Q	=	heat load applied to evaporator
λ	=	latent heat of vaporization
σ	=	liquid surface tension
r	=	pore radius
$()_{liq}$	=	liquid (subscript)
$()_{vap}$	=	vapor (subscript)
$()_{tot}$	=	total (subscript)
$()_{wick}$	=	wick (subscript)

I. Introduction

NASA's science missions are increasingly reliant on high performance thermal control systems to enable operation in extreme environments while providing stability for maximum instrument return. Active two-phase thermal control systems have the potential to enable such missions. These thermal systems also have the potential for dramatic cost reductions for outer planet missions where smaller, non-nuclear powered spacecraft are enabled through higher heat flux accommodation and heater power conservation¹.

In 2015, a technology development program was initiated at JPL to develop technologies that would enable a new class of small (~250 kg) solar powered spacecraft capable of carrying out deep space missions. These spacecraft would use state of the art technologies to minimize the resources (mass and power) needed to achieve science in-line with the National Research Council's Planetary Science Decadal Survey. A crucial task in minimizing the mass and power required for such a spacecraft is the development of an efficient thermal control system. A mechanically pumped two-phase fluid loop was proposed for the thermal control system for this new class of small spacecraft. This benefits of this system were demonstrated through a reference mission study that was developed for a proposed Enceladus orbiter¹.

The efficiency and effectiveness of two-phase thermal systems are well documented^{2,3,4}. Additionally, a two-phase thermal control system has the potential to provide a high degree of isothermality that is crucial for a variety of science instruments such as planet-finding coronagraphs and remote sensing interferometers. There are several benefits of a mechanically pumped system over a passive LHP-type system: A mechanically pumped system offers enhanced flexibility in design (the system is not limited by the capillary head of the evaporator wick), simplified integration (field joints can be utilized and the system can be drained and filled multiple times), and unconstrained testing (the performance is not reliant on system orientation).

The following design and performance requirements for the thermal subsystem were developed for this program¹:

1. Develop a ~1 m² planar heat acquisition zone (evaporator) that can:
 - a. Accommodate up to 500 W
 - b. Accommodate heat fluxes up to 5 W/cm²
 - c. Accommodate distributed, discrete heat loads
 - d. Maintain isothermality within a temperature band of 3 °C across entire evaporator
 - e. Provide temporal stability of less than 0.05 °C /min
2. Use less than 5 W of control power
3. Accommodate multiple evaporators and condensers
4. Provide at least a 15 year lifetime

The first step in developing a viable mechanically pumped two-phase thermal control system was to select a system architecture. Many different architectures have been proposed for mechanically pumped two-phase thermal control systems^{4,5,6,7,8,9,10}, however they can all be classified as either separated flow systems or mixed flow systems⁴. In mixed flow systems, two-phase flow exits the evaporator with the thermodynamic quality varying with heat load. In separated flow systems the liquid and vapor phases are kept separated in dedicated liquid and vapor lines. The phases can be separated in different ways. In this paper a relatively simple separated flow architecture is investigated along with a basic mixed flow architecture.

II. Overview of the Mixed Flow and Separated Flow Architectures

Two different system architectures were explored in light of the requirements outlined above: A Mixed Flow Architecture (MFA) and a Separated Flow Architecture (SFA). A schematic of these two architectures in their simplest form is shown in Figure 1. Both architectures contain the same basic elements: A pump (to circulate the working fluid), an evaporator (to pick up the heat load), a condenser (to reject the heat load), and an accumulator (to regulate system pressure).

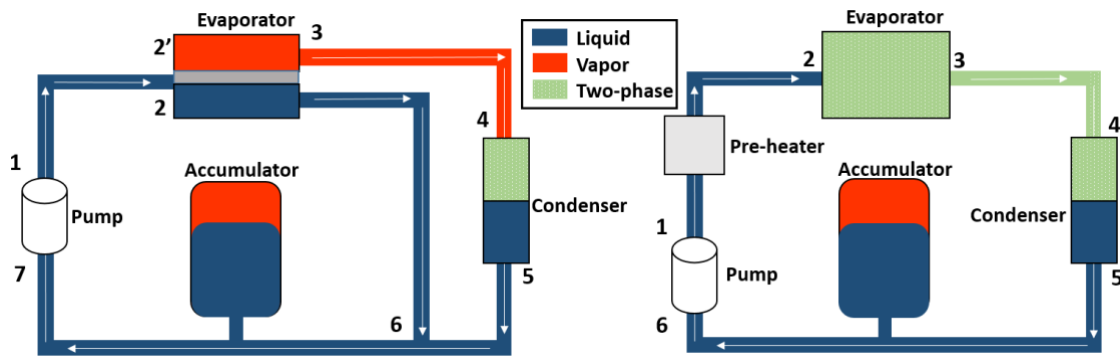


Figure 1. Schematic of a basic Separated Flow Architecture system (left) and a Mixed Flow Architecture system (right). The fluid flows in the direction of the ascending numbers.

The primary difference between the two architectures lies in the design of the evaporator. In the SFA, the evaporator additionally functions as a phase separator and has two outlets: one for vapor and one for liquid. The evaporator is arranged like an LHP evaporator where there is a liquid chamber and vapor chamber that are separated by a porous element (wick) which maintains the liquid-vapor interface. The evaporator acquires heat through the vapor chamber side by evaporating fluid at the liquid-vapor interface. In the MFA, the vapor and liquid phases are not separated in the evaporator and consequently two-phase flow occurs both in the evaporator and in the flow line between the evaporator and condenser. In its simplest form the MFA utilizes flow boiling in the evaporator. Figure 2 schematically illustrates basic forms of the SFA and MFA evaporators. The difference in evaporator design between the two architectures leads to significant operational differences. Note that instead of using a traditional flow boiling configuration, the MFA evaporator for this work also utilized a wick structure.

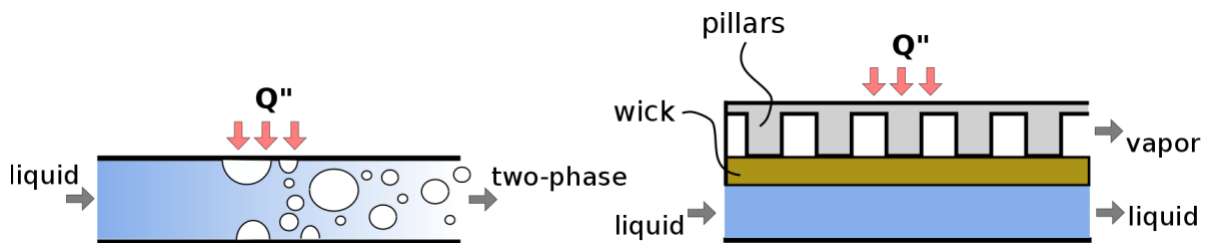


Figure 2. Schematic of basic MFA evaporator (left) and SFA evaporator (right). In its most basic form, a MFA evaporator uses flow boiling. The SFA evaporator is similar to a LHP evaporator with the liquid and vapor separated by a wick structure.

A. Brief Comparison of the MFA and SFA Architectures

At first glance the mixed and separated flow architectures look relatively similar—they are both pumped two-phase loops and have the same basic components. However, once the program goals and details of operation and design are considered, the systems become increasingly distinct, and the SFA begins to look more attractive.

Perhaps the strongest differentiator between the two architectures comes from the implicit requirement for any flight-worthy system that the system be robust and amenable to analysis. Two-phase flow in microgravity is notoriously unpredictable¹¹, especially for the lower flow rates that would be expected to be seen in a 500 W two-phase system where minimal pumping power is required. For low flow rates, inertia forces cannot be guaranteed to dominate over surface tension forces. In the MFA the evaporator and the line between the evaporator and condenser are filled with two-phase flow. This leads to a host of potential flow instabilities that could result in multiple problems like large variable pressure drops or flow maldistribution². These uncertainties and their concomitant issues are obviated in an SFA system. In the SFA the liquid and vapor are separated throughout the evaporator and the transport line between the evaporator and condenser. The location of the phase interface in the evaporator is passively controlled by the porous wick in the evaporator, and the only region with two-phase flow is in the condenser. During steady state operation, the possibility of two-phase flow instabilities forming is greatly reduced.

Another differentiator between the two architectures comes from the requirement for the system to operate upwards of 15 years. Based on current technology, the only type of pump recommended for long-life missions is a centrifugal-style pump with hydrodynamic bearings². A characteristic of these pumps is that they require significant NPSH. This means that the liquid at the pump inlet must be significantly subcooled to avoid cavitation within the pump. (Additionally, the spacecraft environment may lead to significant subcooling). This subcooled liquid will ultimately be transferred to the evaporator inlet (see Figure 1). For the MFA, having subcooled liquid at the inlet of the evaporator makes meeting the isothermally requirement challenging, since the subcooled liquid could come into contact with the heat acquiring surface. To overcome this, the liquid at the evaporator inlet must be pre-heated. This could be done by adding either a recuperating heat exchanger between the lines at the evaporator inlet and outlet, or adding a pre-heater upstream of the evaporator inlet. At best this means additional mass and complexity, at worst it means using additional control power as well. In the SFA design, no pre-heater is required and it is possible for the evaporator to function with sub-cooled liquid entering at the inlet. This is because the heat acquisition surface is never directly in contact with the liquid at the evaporator inlet. Instead the heat acquisition surface is separated from the incoming liquid by the vapor chamber and a wick. The liquid that enters the evaporator must travel through the wick before it reaches the heat acquiring surface. As it travels through the wick it gets pre-heated until it becomes saturated at the liquid-vapor interface. This is the same processes that occurs in an LHP³. This feature of the SFA potentially removes the need for any kind of additional pre-heater.

A few other apparently promising traits of the SFA are that it seems to be relatively simple; it appears to be amenable to the addition of multiple evaporators and condensers; and it has the potential to keep some level of performance even if the pump fails. In principle, if the pump fails, the SFA could function as a CPL, assuming the physical layout is not beyond CPL limits. In this mode, the evaporator would also serve as a CPL pump and would circulate fluid between the evaporator and the condenser. The fluid would flow out of the evaporator vapor line into the condenser and then back to the evaporator through the line that, in normal operation, carries liquid out of the evaporator. Clearly this operational mode would have to be planned for in the system design if it were desired.

III. Evaporator Design

In any two-phase system, the evaporator is a crucial component. It plays a large role in determining the thermal characteristics of the system and strongly influences the design of the rest of the system. For this technology development program, the demanding requirements on the evaporator make it all the more important. As mentioned in the introduction, the primary requirements are to produce a planar 1 m² heat acquisition surface that can remain isothermal (within a 3 °C band) and can accommodate any arrangement of heat loads totaling less than 500 W, with peak fluxes of 5 W/cm². Temporal temperature fluctuations should be less than 0.05 °C/min.

To achieve the programmatic goals, the evaporator concept for both the MFA and SFA was developed based on an LHP evaporator³. Nearly identical sub-scale evaporators were used for both the MFA and SFA testbeds. This was done to facilitate the comparison and to develop a greater understanding of the evaporator concept. The basic layout of the evaporator consisted of a vapor channel and liquid channel separated by a porous wick. In principle, this architecture is well suited to producing an isothermal heat acquisition surface since during nominal operation only vapor (close to the saturation temperature) is present in the vapor channel. Any subcooled liquid is kept away from the heated surface by the wick. This configuration was adapted to a planar geometry to be consistent with the requirements. A sandwich type construction was the result, with the liquid channel, porous wick, and vapor channel

being planar regions that are stacked on one another. This design was first described by Sunada et al¹. Note that the MFA evaporator design used here is actually closer to an SFA-type evaporator—it is not a classic MFA design.

Figure 2 (right) shows a cross-sectional schematic of the evaporator that illustrates the principle of operation. The evaporator consists of a single chamber that is divided by a porous wick. The wick is pressed against pillars which are connected to the heated surface. These pillars transfer heat to the wick and cause evaporation of the working fluid at the pillar/wick interface. During ideal operation, vapor is formed on the pillar side of the wick and flows downstream toward the evaporator outlet. On the other side of the wick, liquid flows from the evaporator inlet to the outlet in a parallel path. In the MFA, liquid and vapor streams are separated by the porous wick until they recombine near the outlet of the evaporator. In the SFA, the liquid and vapor streams remains separated throughout the entire evaporator. The wick serves two primary purposes: (1) it ensures that the heated surface remains wetted in a microgravity environment (to avoid dry out), and (2) it helps keep the heated surface isothermal by constraining the vapor flow to be next to the heated surface. For the SFA design, it has the additional function of serving as a phase separator.

A secondary goal was to design the evaporator such that it would be easy to fabricate. The final design consisted of three primary parts: the evaporator body (incorporating the liquid and vapor chambers with pillars), a sintered steel wick (to separate the liquid and vapor chambers), and a cover plate to close out the liquid chamber. Springs placed between the wick and cover plate were used to ensure good thermal contact between the wick and pillars. An o-ring with a bolted flange was used to provide a seal between the cover plate and the evaporator body. Figure 3 shows drawings of the MFA and SFA evaporators. In order to accommodate the MFA architecture, the liquid and vapor channels were merged at the outlet of the evaporator. For the SFA evaporator, the wick was extended to completely separate the two channels. The external measurements of the prototype evaporators was 254 mm x 216 mm x 254 mm. The casing was made out of aluminum; a stainless steel wick was used that measured 6.35 mm thick, and had a 60 μm effective pore size and porosity of 0.34.

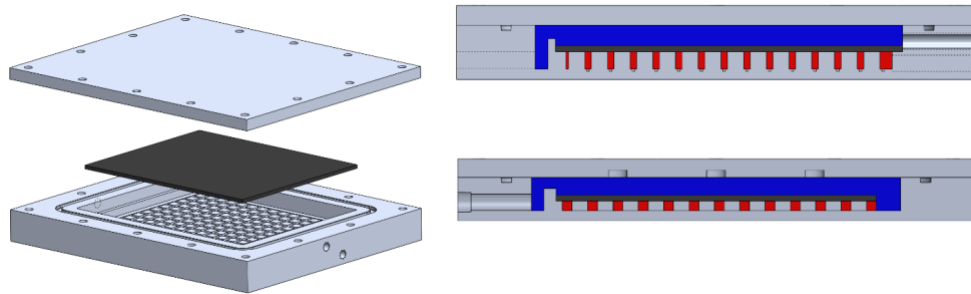


Figure 3. Section view of the evaporator design for the MFA (right– top) and SFA testbeds (right – bottom). The casing (left) for both evaporators was very similar. The vapor channel (red), is separated from the liquid channel (blue) by the wick (black).

IV. Mixed Flow Architecture

MFA systems are the typical mechanically pumped two-phase systems. They are commercially available for ground based systems^{13,14} and have also been developed for use in spacecraft^{4,9,10}. An MFA is currently being used for the thermal control system of an ISS science payload⁹. In these systems, the pump, evaporator and condenser are plumbed in series in a single circuit (see Figure 1-right). Liquid flows from the pump to the evaporator where heat is added to form a two-phase flow. A pre-heater at the inlet of the evaporator is often used to bring the working fluid up to the saturated state^{4,9,10}. Heat is rejected from the

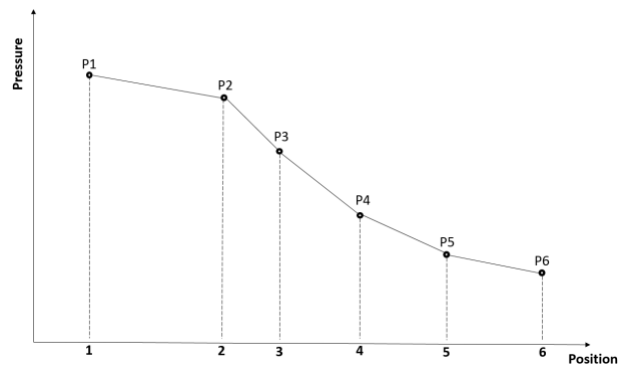


Figure 4. Pressure vs. position for an MFA system (numbers correspond to schematic locations in Figure 1)

flow in the condenser, which outputs sub-cooled liquid back to the pump. The evaporator typically utilizes some form of flow boiling^{4,9,13,14}.

Figure 4 schematically shows a plot of pressure versus position for a basic MFA system (see Figure 1 – right). The pressure monotonically decreases from the pump outlet to the pump inlet. The largest pressure drop is in the portion of the system with two-phase flow (from evaporator inlet (2) to condenser outlet (5)). The pressure drop in the liquid lines is relatively small since flow rates are relatively low and the flow is single phase.

A. Mixed Flow Testbed

In order to experimentally evaluate an MFA system, a simple MFA testbed was designed and built. The goal of the testbed was to enable experimental studies to be carried out in order to better understand MFA systems. Figure 6 shows a schematic of the system along with an image of the fabricated testbed. The working fluid was circulated in a closed loop through a pre-heater, evaporator and condenser. An accumulator was used to regulate system pressure. The pre-heater consisted of electrical heaters mounted to a cold plate. A flat plate liquid-liquid heat exchanger connected to a chiller was used as the condenser/subcooler. The accumulator consisted of a sample cylinder located at the high point of the physical system. The sample cylinder was partly filled with liquid when the system was charged; its orientation with respect to gravity and high location, ensured that the accumulator remained filled and able to regulate system pressure. Accumulator pressure was either controlled by pre-pressurizing the accumulator with air, or by evacuating the vessel and operating it as a saturated liquid/vapor system. In this case the accumulator pressure was controlled by controlling the temperature using a heater/controller circuit. Plumbing to the accumulator was arranged such that it could be used to fix the pressure either near the evaporator inlet or near the pump inlet. Typically the accumulator is placed at the pump inlet to ensure that the NPSH requirement is met, however it was thought that by placing it near the evaporator, temporal thermal stability might be able to be better enforced. A gear pump was used to circulate the fluid.

The loop was instrumented to read fluid temperatures and pressures in multiple locations. Flow rate was measured near the pump outlet. Sight glasses installed at the evaporator inlet and outlet were used to visually monitor the thermodynamic quality of the flow. All transport lines were made of 6.35 mm (0.25 in) stainless steel pipe. Water was used as the working fluid for simplicity. The evaporator described above (section III) was used in the testbed. This system was first described by Sunada et al¹.

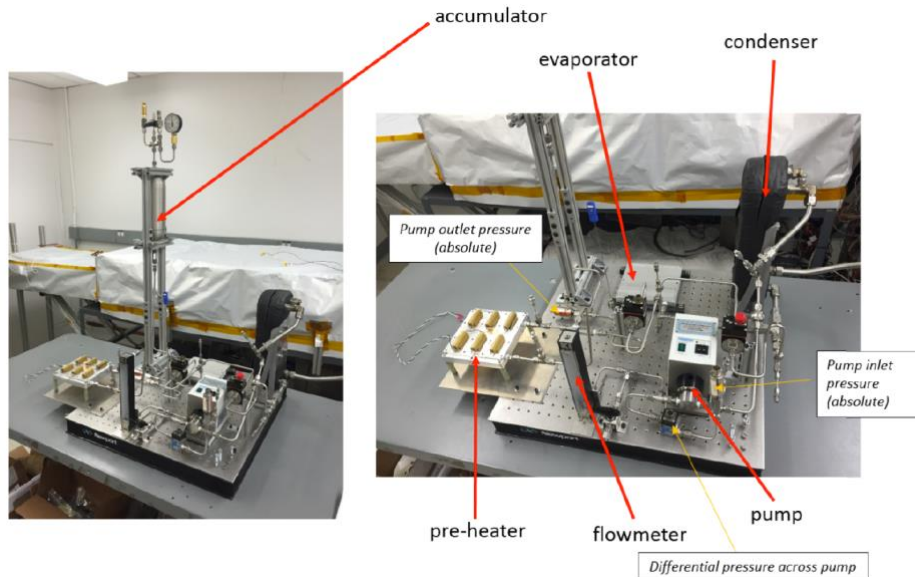
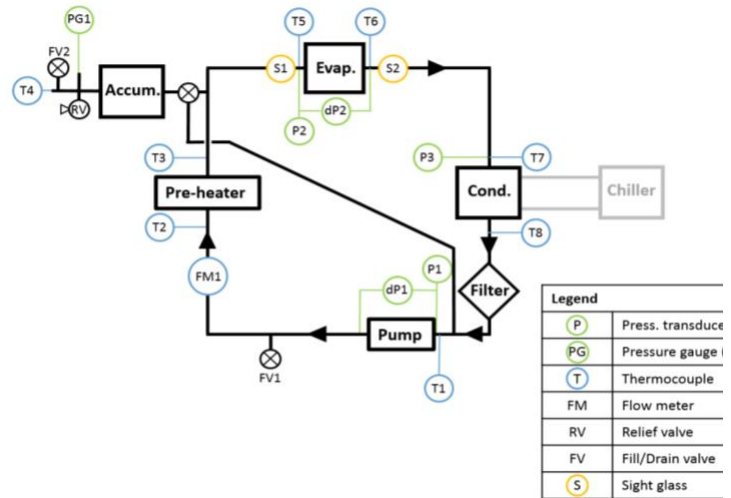


Figure 5. The MFA testbed schematic (top) and testbed (bottom) [1a].

B. MFA Test Campaign

The MFA testbed was used to experimentally explore the potential of an MFA system and to characterize the evaporator design described above. Multiple parameters were varied including flow rate, transport line hydraulic resistance, and evaporator orientation with respect to gravity. Flow rate was modulated via changing the pump speed, transport line resistance was varied using an inline needle valve, and the level of preheat was varied using electrical heaters. Changing the evaporator orientation required reinstalling the evaporator in a new orientation. Changing the accumulator position entailed opening and closing the correct valves. The primary focus of the test campaign was to try and meet the program requirements set forth for the evaporator and system (see Introduction, section I). A secondary focus was to gain an understanding of the evaporator dynamics and of an actual MFA system. An experimental system inevitably reveals idiosyncrasies that are missed in an analytical or computational model.

During the course of the test campaign, operational settings were found that yielded a fairly isothermal evaporator for a range of heat loads. However, to achieve this required significant heat input in the pre-heater to bring the fluid close to saturation. As expected, the evaporator was unable to maintain a tolerable level of isothermality if the fluid at the inlet was significantly subcooled.

Several other findings were made in the course of testing: It was found that the accumulator can produce flow instabilities if it is located near the evaporator inlet, and that the evaporator was able to operate with the vapor side facing either down or up. A more detailed discussion of these findings is given below. Throughout the testing, system pressure was maintained between 4 psia and 6 psia to ensure sufficient NPSH for the pump. The liquid return line (exiting the condenser/subcooler) was always subcooled to 20 °C

1. Steady State Operation with an Isothermal Evaporator

System parameters were adjusted in order to try and maintain an isothermal evaporator with a range of heat loads, in accordance with the program goals. The accumulator was positioned at the evaporator inlet and flow resistance upstream of the evaporator was increased (using the needle valve) to ensure flow stability. The accumulator pressure was set by reducing the air pressure in the head space of the accumulator to about 2.5 psia. The flow rate was fixed at 50 mL/min. 140 W were applied to the pre-heater to bring the fluid temperature from about 21 C up to 60 C at the evaporator inlet. Four different heat loads were sequentially applied to the evaporator: 200 W, 250 W, 300 W and 395 W. The heater measured approximately 6.5 cm by 15 cm and covered about 17% of the evaporator surface. The evaporator was oriented vapor side down. In principle, this is the more challenging orientation for isothermality since the vapor will tend to rise away from the heated surface due to buoyancy. Key temperatures and pressures were recorded around the loop, and IR images of the evaporator were continually acquired.

Figure 6 shows select temperatures and pressures in the loop over the course of the experiment, as well as the heat loads applied to the evaporator. The pump was turned on at about 0.25 hr. At 1.25 hr, 140 W were applied to the pre-heater. At 2.9 hr, the evaporator heater was powered to 200 W. The evaporator heat load was subsequently increased to 250 W (5 hr), 315 W (7.1 hr) and then 390 W (7.25 hr).

Over the course of the experiment, the accumulator pressure increased both gradually and suddenly. The pressure increases are mostly due to the volume of air in the accumulator being compressed as the fluid in the loop expands. The primary fluid expansions occur when the pre-heater is turned on (1.3 hr), when the initial heat load is applied to the evaporator (2.9 hr), and when the final heat load is applied to the evaporator (7.25 hr). The evaporator heat load produces vapor which leads to a significant increase in working fluid volume. Superimposed on these relatively sudden pressure changes is a more gradual increase in pressure. This is due to the temperature of the gas in the accumulator gradually rising over the course of the test. This was due to the ambient room temperature gradually increasing. The ambient temperature rise is also reflected by the gradual increase in the fluid temperature at the outlet of the condenser/subcooler. These pressure increases are attended by an increase in saturation temperature. This explains the slight increase in the evaporator temperature over the course of the test. For the majority of the test the fluid at the evaporator inlet was approximately 9 C subcooled.

The pressure drop remained fairly constant over the course of the test with a slight decrease when the pre-heater was activated and an increase when the evaporator heat load was increased. The initial decrease near 2 hr was due to a reduction in fluid viscosity as the fluid warmed. The subsequent increases in ΔP were due to the two-phase pressure drop when the evaporator heater was activated or changed.

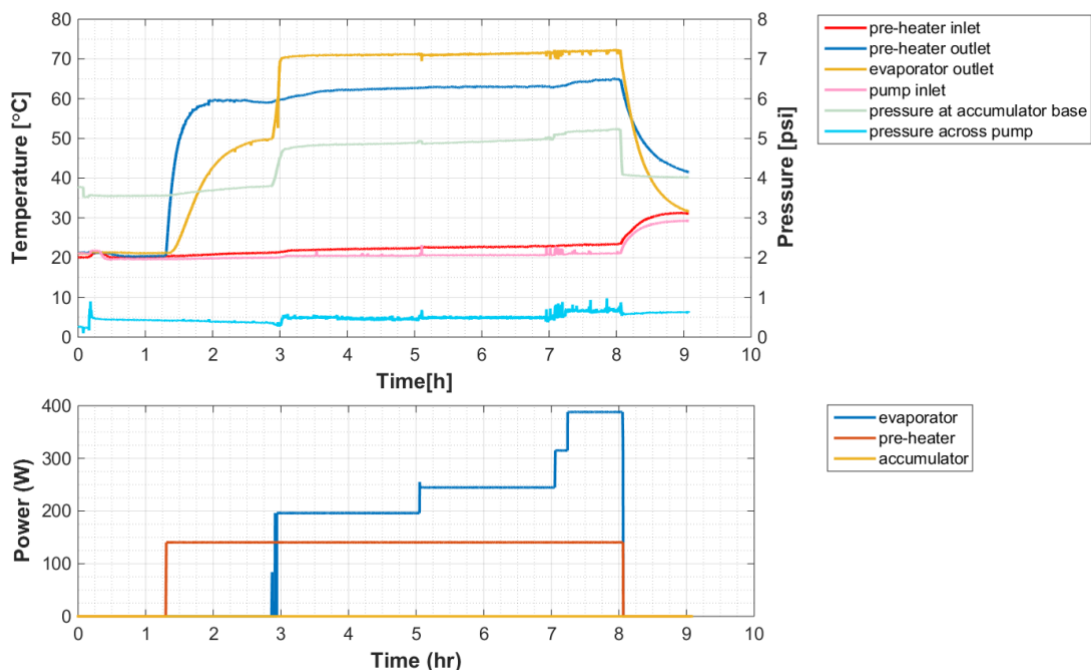


Figure 6. Experimental data for the MFA system set to produce an isothermal evaporator with heat loads ranging from 200 W to 390 W.

The most noteworthy characteristic of the data is that the fluid temperature at the outlet of the evaporator does not significantly change as the heater power is nearly doubled. This is one of the well-touted attributes of mechanically pumped two-phase systems. IR images of the evaporator illustrate this phenomenon even more clearly. Figure 7 shows IR images of the evaporator with three different heat loads. In each case the evaporator is basically the same temperature. These images also highlight the high degree of isothermality attained on the evaporator. The entire surface is within a temperature band of 3 C, although it should be noted that the evaporator is aluminum (highly conductive) and about 1/4 of the target evaporator size. A single phase system using the same working fluid and flow rate would have a temperature difference of 111 C across a heat load of 390 W (using: $Q = \dot{m} \cdot c_p \cdot \Delta T$).

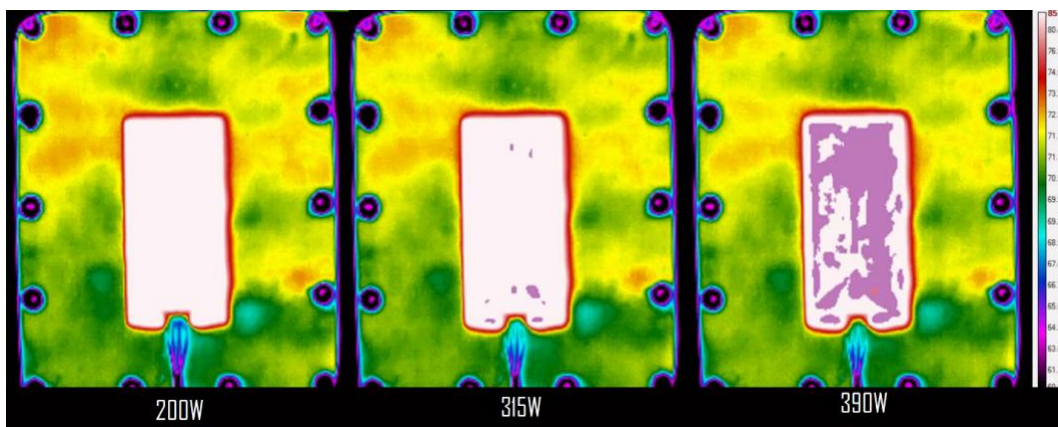


Figure 7. IR images of the MFA evaporator with three different heat loads: 200 W, 315 W, and 390 W. The rectangular shape in the middle of the images is the heater. The evaporator temperature was largely unaffected by the heat load. The heat acquisition surface remained within a temperature band of 3 C.

2. Subcooling Study

One of the concerns with an MFA system is that some form of pre-heater must be used to bring the working fluid up near the saturation temperature. This is done to: (1) ensure two-phase heat transfer in the evaporator and (2) to keep the temperature difference across the evaporator as low as possible. Ideally the entire evaporator is at the saturated temperature, which hopefully varies little over its length. The isothermal capability of the evaporator described above was experimentally investigated by applying several different heat loads and degrees of subcooling. As would be expected, the degree of isothermality is a strong function of the heat load and degree of subcooling.

In the test case described above (section III – steady state isothermal evaporator), a fairly isothermal evaporator was obtained with a heat load varying from 200 W to 390 W and the inlet fluid being subcooled by 9 C. The heater was centered on the evaporator in this case and covered approximately 17% of the heat acquisition surface. A more challenging case is to achieve isothermality when there is a high degree of subcooling, or a small heater is used with a low heat load. This is the case that is discussed below.

In an ideal evaporator, any heat load would produce a layer of vapor which would fill the evaporator's vapor cavity. This would force the entire heat acquisition surface to be near the saturation temperature. This was the goal when this MFA evaporator was designed, however two oversights substantially impaired the evaporator capabilities. One issue stemmed from the fact that the casing was made from a material with a high thermal conductivity (aluminum). The high conductivity makes it hard to decouple the evaporator liquid temperature from the heat acquisition surface, which results in the unwanted cooling of that surface. A potential remedy for this issue is to use a casing material that has a lower thermal conductivity. The other oversight is more fundamental and related to fluid dynamics. The issue arises from the fact that the liquid and vapor chambers are not completely separated. The liquid can flow into the vapor side either through the wick (if there is no liquid vapor interface in the wick to inhibit flow) or through the connecting channel. This was observed to occur during testing and inhibited the ability to maintain an acceptable degree of isothermality when subcooled liquid was present. An additional issue came from the vapor produced by the heat load evidently getting superheated.

A series of tests was conducted where a 2.4 cm x 10 cm heater mounted near the evaporator inlet was used to supply 48 W of heat. The heater covered approximately 10% of the heat acquisition surface. The isothermality of the surface was measured as a function of different levels of subcooling at the evaporator inlet. The degree of subcooling was varied from 10 C to 0.5 C. The isothermality of the evaporator was measured using the temperature difference between a point right next to the heater and a point close to the edge of the vapor cavity by the evaporator outlet. Temperatures were measured using an IR camera. Figure 8 shows an IR image of the evaporator with the line along which temperature was measured. While the temperature gradient decreased as the level of subcooling decreased, it remained appreciable. Even with only 0.5 C of subcooling, the ΔT across the evaporator was found to be 6 C. In the case where the subcooling was 10 C, the ΔT across the evaporator was also 10 C. The temperature gradient was due to two components: (1) The ΔT between the sub-cooled liquid and saturated vapor, and (2) superheating of the vapor near the heater. The latter reason caused the ΔT across the evaporator to be even larger than the degree of subcooling, when the subcooling was relatively small.

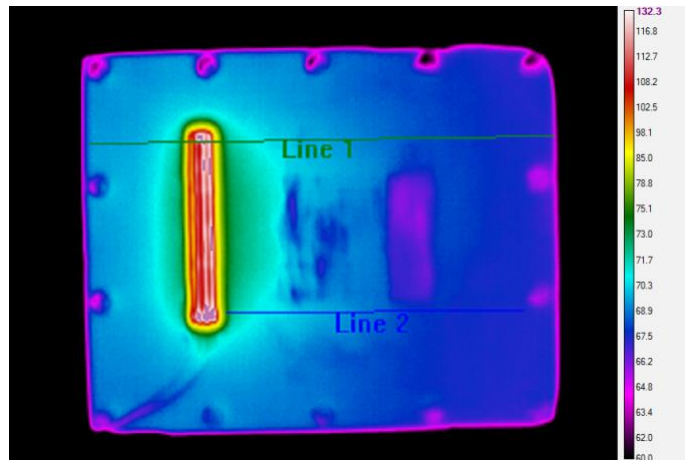


Figure 8. An IR image of the evaporator with a small heater used to study the effect of subcooling on the isothermality of the evaporator. The fluid is flowing from left to right. The heater is the red rectangular element on the left. The blotchy regions in the center-right of the image are due to blemishes in the paint. Temperatures were measured along the lower line shown in the image. The temperature difference between the two end points of the line were used to characterize the isothermality of the plate.

3. Accumulator Position

In mechanically pumped two-phase fluid loops, the accumulator is often located near the inlet of the pump, to ensure sufficient NPSH. However, in principle, locating the accumulator this far from the evaporator could be seen

to be sub-optimal for a system that requires high temporal stability in the evaporator. After all, the operating temperature in the evaporator is ultimately dictated by its saturation temperature, which is in turn controlled by the local pressure. The accumulator provides the control point for the pressure in the loop. If the accumulator were closer to the evaporator, then perhaps it could be used to more directly regulate the evaporator pressure and thus enhance its temperature stability.

With this idea in mind, MFA system testing was done with the accumulator in two different positions: (1) near the evaporator inlet or (2) near the pump inlet. It was found that locating the accumulator near the inlet of the evaporator led to flow instabilities in the form of periodic oscillations in the fluid flow. It was found that these oscillations could be suppressed by increasing the flow resistance between the inlet of the evaporator and the accumulator. This somewhat negated the benefit of situating the accumulator near the evaporator, since the additional resistance inherently creates a separation in pressure between the accumulator and evaporator. Additional details are given below.

When the accumulator was located at the inlet of the evaporator, a flow instability arose soon after a heat load was applied to the evaporator. The flow instability manifested as a periodic oscillation where the system alternated between two different states. In the primary state operation was normal and the fluid flowed in the expected manner; in the secondary state the fluid would flow backwards in the section of the loop between the accumulator and evaporator. That is, the fluid would flow from the evaporator to the accumulator. This was clearly observed in the experiment as vapor could be seen entering the accumulator via a sight glass.

This phenomenon can be explained using a simple flow resistance model. Figure 9 shows a schematic of the MFA system with the flow resistances. During normal operation the pressure monotonically decreases from the pump outlet to the pump inlet ($P1 > P2 > P3 > P4 > P5$). However the instability sets in when the two-phase pressure flow resistance ($R2$) starts to grow as the flow is established. The growing two-phase flow restriction causes the pressure in the evaporator to build as additional vapor is continually produced by the heat load. At some point the pressure in the evaporator ($P3$) becomes larger than the pressure in the accumulator ($P2$), and it becomes easier for the fluid to flow to the accumulator. Analytically, this corresponds to the case when $(P3-P2)/R1 > (P3-P4)/R2$. During the period of backflow the pumped fluid is redirected into the accumulator. This backflow condition can be suppressed by increasing the resistance between the accumulator and the evaporator ($R1$) such that $(P3-P2)/R1 < (P3-P4)/R2$ always. This method of backflow suppression was experimentally confirmed to work; it is in the same vein of instability suppression previously reported².

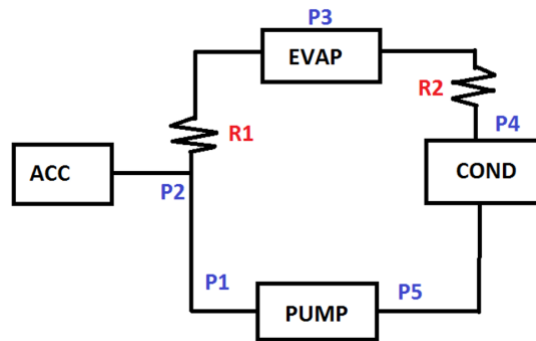


Figure 9. A schematic of the MFA system pressures and flow resistances. During normal conditions, the pressure decreases monotonically from the pump outlet to its inlet. During the backflow condition, pressure is higher in the evaporator than the accumulator ($P3 > P2$) and fluid flows from the evaporator to the accumulator.

4. Evaporator Orientation

The evaporator designed for this testbed incorporates a wick to mitigate the effects of gravity. One of the primary functions of the wick is to ensure that the heated surface stays wetted, regardless of orientation. Dryout of the heated surface is a known issue, especially if the heated surface is facing upwards². Testing was done in order to verify that the wick was functioning as anticipated and was able to keep the heated surface wetted, without vapor penetration. To do this, the evaporator was operated both with the heated surface facing downwards and with the heated surface facing upwards. Results indicated that the wick functioned as anticipated. Dryout was never encountered with the heated surface facing upwards and heat fluxes up to 2.5 W/cm^2 . Additionally, the heated surface was kept within $3 \text{ }^\circ\text{C}$ of the fluid saturation temperature when the heated surface was facing downwards, with subcooled liquid entering the evaporator (see Figure 8). The heat load was at least 200 W and level of subcooling was $9 \text{ }^\circ\text{C}$. This suggests that the wick provided effective phase separation when the heat load was high enough.

V. Separated Flow Architecture

In this section the SFA is presented in more detail. Its mode of operation is outlined, and a basic system model is presented. The model is used to show some theoretical limitations of the architecture as well as to conduct a small working fluid study to show how real systems might be limited. Finally an SFA testbed developed at JPL is presented along with some preliminary findings.

A. Overview

Several variations of mechanically pumped separated flow systems have been investigated in the past^{5,4,6,7,8,15} with varying degrees of reported success. The specific architecture explored here is most similar to that presented in references^{5,6,7,16}. Figure 1 (left) shows the key elements of the architecture. A pump circulates the working fluid, an evaporator absorbs the heat load, and a condenser rejects the heat load. An accumulator is used to set the system pressure at the pump inlet. The evaporator is designed similarly to a CPL evaporator, with liquid and vapor channels being separated by a porous wick (Figure 2-right). Unlike a CPL evaporator, the SFA evaporator has a liquid outlet line that allows the liquid flow to bypass the evaporator and continually circulate during normal operation. This means that during normal operation, excess liquid is not forced through the wick by the pump. Instead, the wick picks up whatever liquid it needs to satisfy the vapor mass flow rate required by the heat load. The vapor and liquid phases remain separated in the entire loop except for in the condenser.

To better understand the architecture, it is useful to consider how pressure varies through the system at steady state. Figure 10 schematically show the pressure in the system as a function of position. These positions correspond to the locations labeled in Figure 1. At the outlet of the pump (1), the pressure is high. Between the pump outlet and evaporator inlet the flow is single phase liquid and pressure decreases monotonically. Inside the evaporator, two distinct pressure regions exist: one in the vapor chamber (2') and one in the liquid chamber (2). These chambers are completely separated by a porous wick that contains the liquid-vapor interface during steady state operation. The application of a heat load maintains the presence of vapor in the vapor chamber. The liquid-vapor interface forms a meniscus that can sustain a pressure difference across it. During normal operation, the pressure in the vapor chamber is higher than in the liquid chamber. This prevents liquid from being forced into the vapor chamber by the pump. Depending on how the system is designed, the vapor pressure in the vapor chamber can be even higher than at the pump outlet. The pressure in the liquid chamber varies relatively little between the inlet and outlet of the evaporator, since the hydraulic diameter here would typically be bigger than in the transport lines. In the liquid bypass line between the evaporator (2) and the point where the liquid and vapor lines meet (5), the pressure drops monotonically due to the flow of liquid. In the vapor line between the outlet of the evaporator (2') and the point where the two flows meet (3), the pressure also monotonically decreases. In the first leg of the line between the evaporator (2') and condenser (3), the flow is pure vapor; in the second section within the condenser (3 to 4) the flow is two-phase; and in the third section from the condenser outlet (4) to the point where liquid and vapor lines recombine (5) the flow is pure liquid. After the two lines meet the flow is liquid up to the pump inlet (6). The pressure at the pump inlet is fixed by the accumulator.

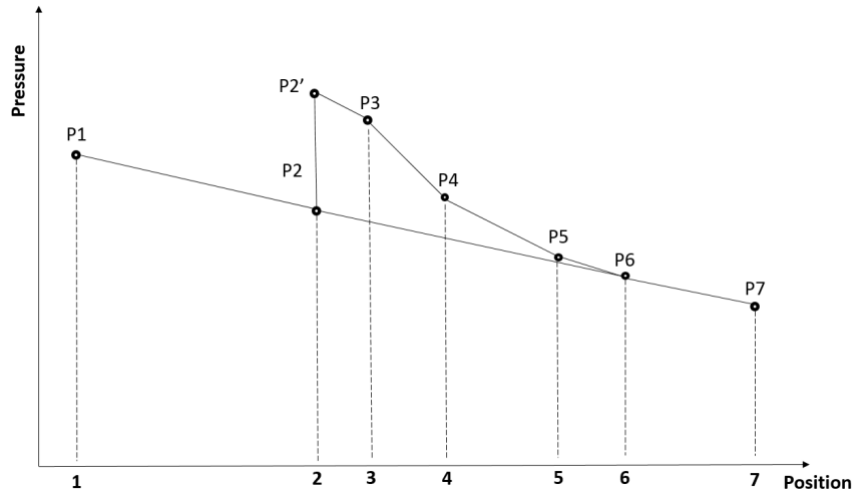


Figure 10. Pressure versus position for a typical SFA system (numbers correspond to Figure 1)

B. Basic Model

In this section a basic lumped parameter model is developed and used to better understand how an SFA system operates and what some of its limitations are.

Consider the portion of a simple SFA system from the evaporator inlet to the point after the condenser where the liquid and condensed vapor lines meet (point 6 in Figure 1). This is the section of an SFA system that is of primary interest. Figure 11 shows two schematics of this section illustrating the physical system and its simplified, abstracted circuit diagram. At steady state, the vapor chamber is filled with vapor as is the line between the outlet of the evaporator and the condenser. The condenser contains two-phase flow, and the remainder of the system contains liquid. The liquid and vapor phases are separated in the evaporator by a meniscus which forms in the wick (just as in a heat pipe). The key physical parameters accounted for in the lumped parameter model are shown on the circuit diagram. Pressure in the liquid chamber and on either side of the meniscus is captured as well as flow resistances in the wick (R_{wick}), liquid chamber (R_{liq}) and vapor chamber (R_{vap}).

Note that R_{liq} and R_{vap} also include the hydraulic resistances of the liquid and vapor lines at the outlet of the evaporator up to the point where the two lines meet (point 2 in Figure 11).

At steady state operation the system can be described with the following equations:

P_i - pressure	$Q = \dot{m}_{vap} \lambda$	(1)
\dot{m}_i - mass flow rate	$\dot{m}_{tot} = \dot{m}_{vap} + \dot{m}_{liq}$	(2)
Q - heat load on evap	$P_1 - P_2 = \dot{m}_{liq} R_{liq}$	(3)
R_i - flow resistance	$P_3 - P_2 = \dot{m}_{vap} R_{vap}$	(4)
λ - latent heat of vap.	$P_1 - P_1' = \dot{m}_{vap} R_{wick}$	(5)

The variables are defined next to the equations and are shown in Figure 11. Equation 1 relates the heat applied to the evaporator to the rate of vapor formation. Implicitly, this equation only accounts for the heat that goes into the vapor—heat that goes into bringing the subcooled liquid up to saturation and heat losses are not included. Equation 2 states the conservation of mass for the system. Equation 3 describes the relationship between pressure drop and flow rate through the liquid chamber of the evaporator and the entire liquid line up to the point where it recombines with the condensed vapor line. Equation 4 describes the pressure drop/flow relationship from the vapor side of the meniscus through the condenser up to where the two flow lines meet. Equation 5 describes the hydraulic flow through the wick from the liquid chamber up to the liquid side of the meniscus. Depending on the flow regime, the flow resistance may be a function of the flow rate. The pressure drop between the inlet of the evaporator and the liquid side of the wick are considered negligible. The model is a lumped-parameter model that assumes the steady-state operation described above.

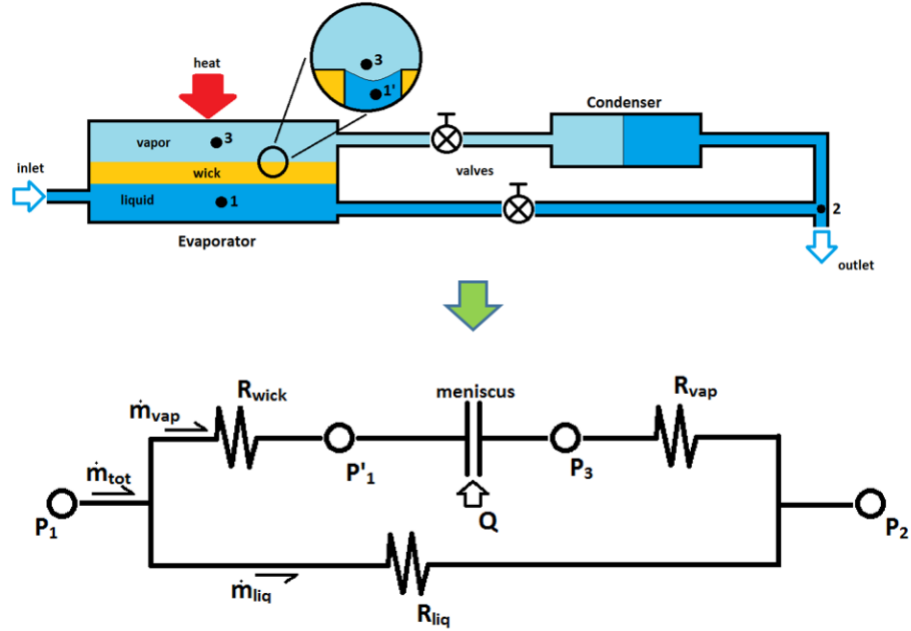


Figure 11. Schematic of the section of the SFA system that is being modelled (above), and the corresponding circuit diagram (below). The circuit diagram visually describes the simplified lumped-parameter model that is developed here. The key quantities of the model are included in the diagram.

To apply the model, the dependent and independent variables must be defined. For an actual system, it would be expected that the total flow rate (\dot{m}_{tot}) is known and controlled. With this information and knowledge of the system, the pressure at the inlet of the evaporator (P_1) is easily found. Similarly the hydraulic resistances of the system would be dictated by the physical geometry and the heat load (Q) would be known. The latent heat of vaporization (λ) would be fixed by the selection of a working fluid. This implies that the independent variables of the model are: \dot{m}_{tot} , λ , Q , R_{liq} , R_{vap} , and R_{wick} . The dependent variables are then \dot{m}_{vap} , \dot{m}_{liq} , P_2 , P_3 , and P_1' . With these stipulations, Equations 1 – 5 form a system of 5 equations with 5 unknowns. The problem is therefore well-posed and has a unique solution.

The model given by Equations 1 – 5 can be used to explore how changes in the independent variables (e.g. \dot{m}_{tot}) affects system performance. Of particular interest is to see how an SFA system compares to a CPL or LHP type system. The fact that the system relies on the capillary head of the wick for operation begs the question of whether this architecture offers any advantage to a CPL or LHP. In a CPL and LHP, the evaporator functions as the pump, and pressure increases across the meniscus from the liquid to the vapor side. This pressure rise adjusts so that it is equal to the pressure drop in the remainder of the system³. One of the classical limits of a CPL/LHP is that the pressure drop in the system must be less than the capillary head available in the capillary pump³. For a capillary pump, the maximum available head is equal to $2\sigma/\tau_{eff}$. This cap on the max allowable pressure drop ultimately limits the allowable heat load, since increasing the heat load increases the mass flow rate which increases the pressure drop. Using the model developed above (Equations 1-5), the pressure difference across the meniscus ($P_3 - P_1'$) can be solved for in terms of the independent (known) quantities. Doing this yields:

$$(P_3 - P_1') = \frac{Q}{\lambda}(R_{vap} + R_{liq} + R_{wick}) - \dot{m}_{tot} R_{liq} \quad (6)$$

Note that unlike an LHP, the pressure across the meniscus is *not* simply equal to the pressure drop across the system—it is a more complex function of flow resistances, the pumped flow rate and heat load. Equation 6 suggests that even the pressure drop across the vapor line is not solely reliant on the capillary head developed across the meniscus. This can be more clearly seen by substituting Eqn. 1 into Eqn. 6 and solving for the pressure drop in the vapor line ($P_3 - P_2$):

$$(P_3 - P_2) = (P_3 - P_1') + \dot{m}_{tot} R_{liq} - \frac{Q}{\lambda}(R_{vap} + R_{wick}) \quad (7)$$

For a given heat load (Q), the vapor mass flow rate \dot{m}_{vap} is fixed as is the pressure drop across the vapor line ($P_3 - P_2$). The pressure head developed to overcome this pressure drop comes from the meniscus ($P_3 - P_1'$) and the pump ($\dot{m}_{tot} R_{liq}$). The burden on the meniscus can be reduced by increasing the mass flow rate put out by the mechanical pump (\dot{m}_{tot}), or by increasing the resistance in the liquid line (R_{liq}). This second effect can be more clearly seen by substituting Eqns. 1 and 2 into 7 and rearranging:

$$(P_3 - P_2) = (P_3 - P_1') + \dot{m}_{liq} R_{liq} - \dot{m}_{vap} R_{wick} \quad (8)$$

While an SFA system is not as reliant on the capillary pumping head as an LHP, it still has limits of operation that stem from the capillary wick in the evaporator. For normal SFA operation, the vapor and liquid in the evaporator must remain separated by the meniscus in the wick. This means that liquid cannot flow into the vapor chamber, and similarly vapor cannot flow into the liquid chamber. In order for liquid to be prevented from flowing into the vapor chamber, the pressure must be higher in the vapor chamber than in the liquid chamber. However, in order to ensure that vapor does not penetrate the wick and enter the liquid chamber, the pressure across the meniscus cannot exceed the available capillary pressure head: $2\sigma/\tau_{eff}$. If the available capillary pressure is exceeded, vapor will push back the meniscus and flow into the liquid chamber. These requirements on pressure can be formalized as:

$$0 < (P_3 - P_1') < \frac{2\sigma}{r} \quad (9)$$

This equation states that the pressure difference across the meniscus must be less than the maximum available capillary head and greater than zero. Substituting Equation 6 into equation 9 and rearranging yields limitations on the allowable heat load (Q) for a given system:

$$\frac{\lambda(\dot{m}_{tot}R_{liq})}{(R_{vap} + R_{liq} + R_{wick})} < Q < \frac{\lambda(2\sigma/r + \dot{m}_{tot}R_{liq})}{(R_{vap} + R_{liq} + R_{wick})} \quad (10)$$

If the heat load is less than the minimum allowable value $\lambda(\dot{m}_{tot}R_{liq})/(R_{vap} + R_{liq} + R_{wick})$, liquid will enter into the vapor chamber; if the heat load is greater than the maximum allowable value $\lambda(2\sigma/r + \dot{m}_{tot}R_{liq})/(R_{vap} + R_{liq} + R_{wick})$, vapor will enter the liquid chamber. As alluded to previously the maximum allowable heat load is not solely limited by the available capillary head of the wick $2\sigma/r_{eff}$ as in an LHP. Instead it is also a function of the hydraulic resistances in the system, the latent heat of the working fluid, and the mass flow rate produced by the pump. The max allowable heat load can be increased in a few different ways: by decreasing hydraulic resistances in the system or by increasing the mass flow rate put out by the pump. This gives the SFA a system level advantage over an LHP or CPL: the max allowable heat load is not solely dictated by the capillary wick.

With some clear limitations on system performance defined by the model, it is natural to ask how a real system might be limited. To do this, the maximum and minimum allowable heat loads were calculated for a specific set of system parameters (line length, fluid properties, flow rate). The system was assumed to have a liquid line of 5 m (from the evaporator liquid outlet to the point where the liquid and vapor line recombined); the vapor line was assumed to be 15 m (from the evaporator vapor outlet through the condenser up to the point where the liquid and vapor lines meet). The internal diameter of all lines was assumed to be 9.52 mm (0.375 in). The effective pore size of the wick was assumed to be 60 μm and the permeability was assumed to be $4 \times 10^{-11} \text{ m}^2$. Fluids were assumed to be perfectly wetting. Hydraulic resistances were calculated using either a laminar or turbulent model as appropriate. The flow rate was held constant at 200 mL/min. Fluid property data was taken from NIST refprop¹⁷ assuming an operating temperature of 20 °C. The results for 26 different fluids are shown in Table 1.

Of course other practical limitations may constrain an SFA system more than the constraints defined in Equation 10, however these constraints give an initial filter to see how a real SFA system using different fluids might be limited. In Table 1, several fluids look promising from an allowable heat load perspective including some common refrigerants and heat pipe fluids such as ammonia and propylene. Surprisingly water does not offer very good performance. This is because the latent heat is not the only property that matters—other properties that enter into the hydraulic resistance are important as well (liquid and vapor viscosity and density).

C. Separated Flow Testbed

A testbed was designed and developed and built to experimentally explore a SFA. SFA systems are somewhat unconventional and have not been thoroughly investigated in the literature. This gives rise to a degree of uncertainty

Table 1: Range of allowable heat loads for a prototypical SFA system for different working fluids. Based on Equation 10.

Fluid	Q_{\min} (W)	Q_{\max} (W)
Ammonia	217.6	1559.2
Butane	103.4	438
1-Butene	101.4	450.2
Dimethylether	109.5	568.5
Hydrogen sulfide	155.2	861.1
Isobutane	111.8	416.2
Isobutene	102.6	449.2
Propane	141.8	492.1
Propylene	147.8	525.5
Propyne	126.5	587.7
R115	67.8	278.2
R12	70.1	383.1
R1234	74.8	344.1
R1234ZE	80.1	411
R124	125.5	542.6
R134A	86.7	427.1
R142	104.4	507.6
R143	90.4	351.8
R152A	99.2	492.2
R161	116.2	565.1
R218	65.1	245.8
R22	85.5	460.5
R227EA	95.1	402.5
R32	104.5	518.4
Sulfur dioxide	136.5	953.5
Water	9.2	65.3

regarding the operation of SFA systems both in principle and in practice. The goal of the SFA testbed was to reduce these uncertainties and develop an understanding for how these systems operate.

A schematic of the SFA testbed is shown in Figure 12. A centrifugal pump circulates the working fluid sequentially through a pre-heater, evaporator, condenser, and subcooler. The flow is split into two parallel paths in the evaporator where the heat load is applied. One path is used for vapor transport and the other for transporting liquid which bypasses the evaporator. After the vapor flow is condensed in the condenser, the two streams reunite to pass through the subcooler. Other components include a gas trap to capture non-condensable gases, a filter to protect the pump, and an accumulator to control system pressure. The plumbing for the accumulator was setup so that the accumulator position could be changed between the evaporator inlet and the pump inlet. Multiple needle and ball valves were incorporated to facilitate maintenance operations and vary operational conditions. The system was instrumented to read fluid temperatures, pressures and flow rates in multiple locations around the loop. Water was used as the working fluid for convenience.

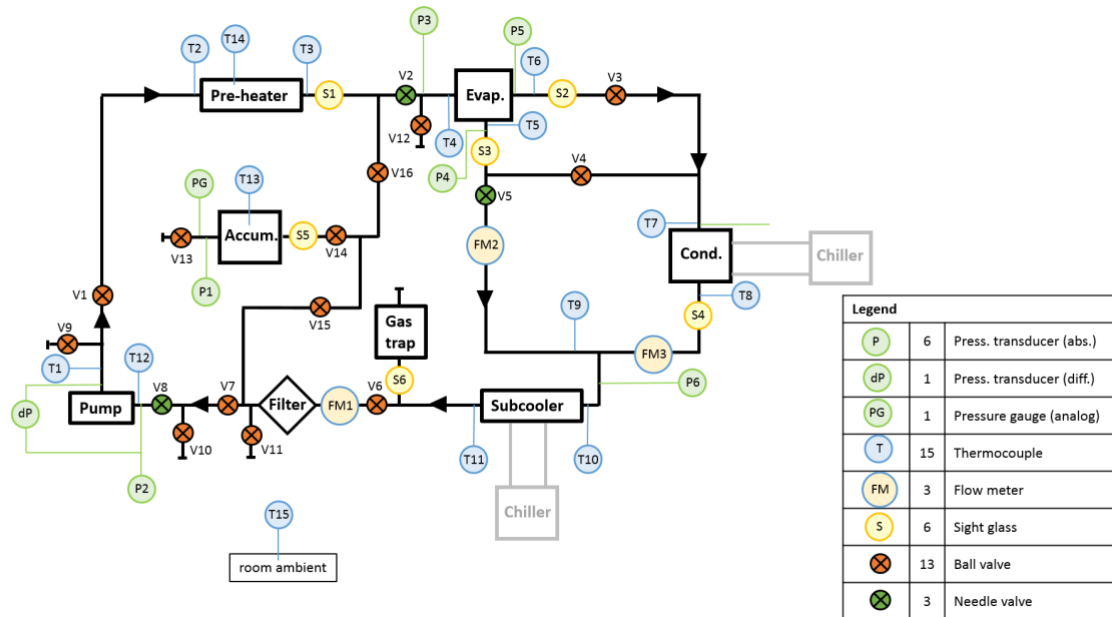


Figure 12. Schematic of the SFA testbed



Figure 13. The separated flow testbed prior to insulation.

Most of the components used were commercial off-the-shelf parts. A miniature centrifugal style pump was used to circulate the fluid. A high efficiency cold plate mounted with heaters was used as the pre-heater. Brazed plate heat exchangers were used as the condenser and subcooler. A custom accumulator was built to enable temperature control for saturated fluid pressure regulation. The accumulator was essentially a shell and tube heat exchanger, where the shell side was attached to the SFA system and the tube side circulated fluid from a temperature controlled chiller. This enabled the temperature control of the accumulator, which also dictated pressure for this saturated system. Figure 13 shows the fabricated testbed. The system was insulated to thermally isolate it from the environment. The evaporator described above (Section III) was used in the testbed.

D. SFA Test Campaign

A test campaign was carried out utilizing the testbed described above. Operational parameters were varied such as: flow rate, evaporator heat load, degree of pre-heating, and the method of pressure control in the accumulator. The general goal of the testing was to develop an understanding of how the system behaves. Additionally, the system stability was investigated by perturbing the system and observing whether it could regain stable operation. The condenser temperature and heat loads were varied along with the pump operation. Over the course of testing the following points were demonstrated:

1. A stable separated flow system is possible
2. A pre-heater is not required for an SFA system
3. The SFA system is stable and robust
 - a. Evaporator performance was insensitive to fluctuations in condenser temperature of 10 °C (0.8 °C/min rate)
 - b. The system could recover from excessive/insufficient heat loads, the pump stopping, and the condenser stopping to function for temporary periods.

1. Nominal Operation

Stable system operation with the SFA testbed was demonstrated for two different flow rates and a range of heat loads. It was found that the pre-heater was not needed. During stable operation, separated flow was established in the system with vapor filling the vapor line and liquid filling the liquid line. Stable, separated flow was only achievable for a range of heat loads. If the heat load was too low, liquid was seen in the vapor line; if the heat load was too high, vapor was seen in the liquid line. This is consistent with the theoretical findings shown above (section V), and has also been observed by other investigators^{5,16}. Additionally, it was found that higher flow rates could accommodate higher heat loads. This is also consistent with the theory presented above. Table 2 shows the range of allowable heat loads established for two different flow rates for the SFA testbed using water as the working fluid.

Table 2. Range of allowable heat loads for stable separated flow in the SFA testbed.

Flowrate (mL/min)	Range of heat loads for completely stable operation (W)
50	225 - 250
79	275 - 350

Figure 14 shows test data from the SFA testbed at stable operation. The flow rate was 79 mL/min and no pre-heater was used. System pressure was held at 5 psia at the pump inlet using a temperature controlled, saturated accumulator. The evaporator saturation temperature was 68 °C; the subcooler was set to output fluid at 21 °C. The evaporator heat load was set to 350 W for the entire test except from 2.25 hr to 4 hr, when the heat load was 275 W. The flow remained separated over the course of the test. This was verified by observing sight glasses placed at the evaporator outlets, and was corroborated by the fact that the evaporator liquid outlet temperature was subcooled, while the vapor outlet temperature was saturated.

Promising features of this data are: (1) The temperature at the evaporator outlet does not significantly change with heat load, as expected; (2) the flow remains separated with the liquid at the liquid outlet of the evaporator remaining subcooled and the vapor at the vapor outlet remaining saturated; (3) No pre-heat is needed for stable operation, even with the fluid entering the evaporator 50 °C subcooled. These features demonstrate the stable operation of the SFA testbed, and its potential to provide performance without a pre-heater.

Two less promising features of the data are: (1) the liquid on the liquid side of the evaporator increases in temperature by about 45 °C from the inlet to the outlet, and (2) the outlet vapor temperature becomes a little more noisy when the lower heat load is applied (275 W). The increase in temperature of the liquid flow in the evaporator indicates significant heat transfer to the liquid and that the liquid and vapor sides are thermally well-coupled. Using $Q = (\dot{m} \cdot c_p \cdot \Delta T)$, the heat loss during this experiment was estimated to be 173 W or 49 % of the applied heat load. This strong thermal connection between the liquid and vapor sides inhibits the performance of the evaporator in two ways. Firstly, it prevents the evaporator from reaching any reasonable degree of isothermality for small heat loads, if the fluid is entering highly subcooled. In this case the temperature of the cold liquid cools the top surface of the evaporator near the liquid inlet and the temperature gradient across the heat acquisition surface becomes untenable. In the same vein, the heat that is lost to the liquid side would otherwise be used to produce more vapor which would make it more likely to fill the vapor cavity with vapor. Filling the vapor cavity with vapor is a pre-requisite for an isothermal evaporator. Secondly, when the heat transfer path to the liquid is too large, boiling can occur in the liquid side of the evaporator. This can prematurely limit the maximum allowable heat load that would otherwise be possible. For these reasons decoupling the liquid and vapor regions is crucial for good performance of the evaporator. The current evaporator was not designed to minimize this thermal coupling, since its importance was not initially realized.

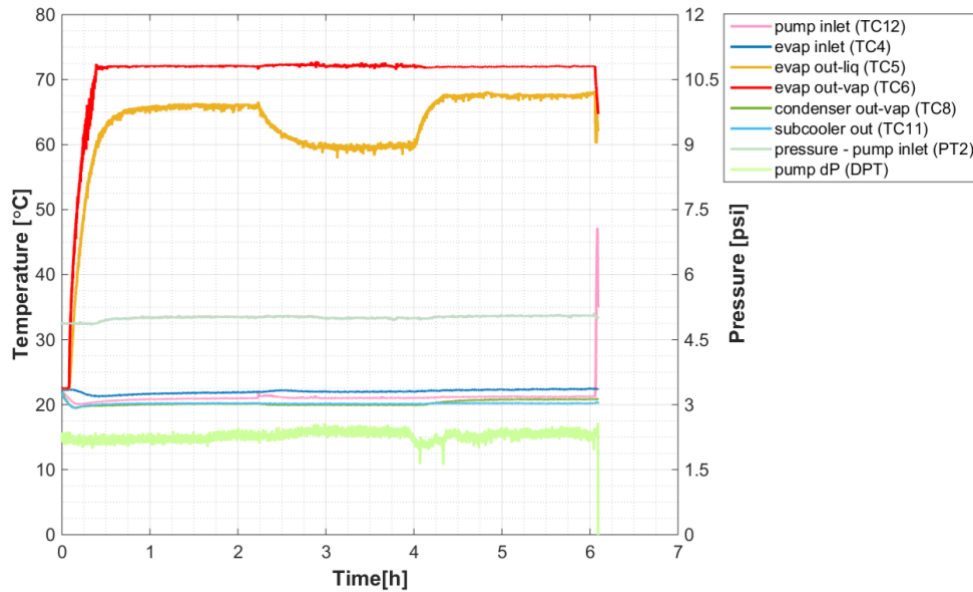


Figure 14. Experimental Data from the separated flow testbed.

2. System Stability

The stability of the SFA testbed was investigated by establishing a stable operating condition (with stable separated flow), and perturbing it. Methods of perturbing included: stopping the pump, varying the condenser temperature, exceeding the max allowable evaporator heat load, or applying a heat load below the minimum allowable heat load for stable operation. In all these cases the system was able to consistently recover once the nominal operating conditions were restored.

Figure 15 shows test data incorporating four different perturbations. Steady separated flow was initially established in the testbed with a flow rate of 79 mL/min and an evaporator heat load of 350 W. The accumulator was located at the pump inlet. After stable operation was established (0.8 hr), the perturbation sequence was initiated. This consisted of forcing a known operating condition that resulted in the loss of steady separated flow and then restoring the initial nominal operating conditions. In each case, the testbed reverted to its initial stable state once the nominal operating conditions were restored. At 1 hr the evaporator heat load was increased to 450 W—this resulted in the loss of separated flow with vapor exiting the liquid outlet of the evaporator. At 2.8 hr, the evaporator heat load was shutoff—this resulted in liquid exiting the vapor outlet of the evaporator. At 4.7 hr, the condenser chiller was turned off—this eventually resulted in vapor exiting at the liquid outlet of the evaporator. At 6.4 hr, the pump was turned off—this resulted in vapor being pushed out of all ports of the evaporator and the evaporator wick drying out.

In between each of these perturbation events, the system was restored to a stable steady operating point by restoring the initial conditions. No hysteresis effects or flow instabilities were observed.

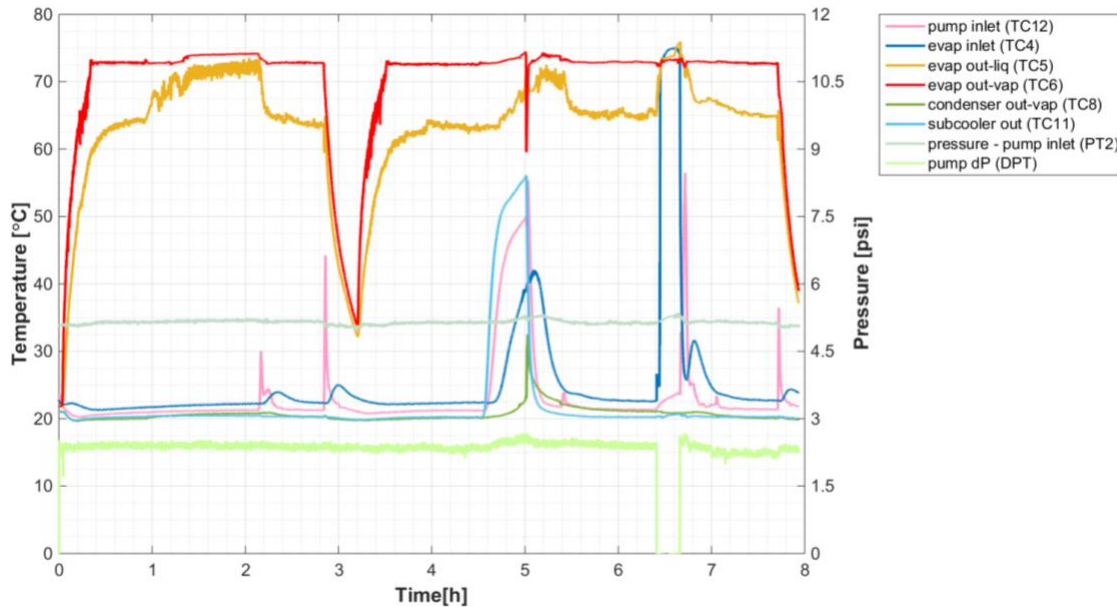


Figure 15. The separated flow system undergoing stability testing. The system was perturbed by exceeding the max heat load (1 hr); shutting off the heat load (2.8 hr); shutting off the condenser chiller (4.7 hr); and turning off the pump (6.4 hr). In each case the system was able to recover when the nominal operating conditions were restored. This is demonstrated by the restoration of the nominal operating conditions initially established by 0.6 hr.

3. Evaporator Performance

The SFA evaporator was able to produce separated flow and verify the operation of the separated flow architecture. However it was unable to meet the programmatic requirements for thermal performance, namely isothermality. It became clear that the evaporator was unable to meet isothermality requirements with a localized heat load. It was only possible to get the isothermal area to extend slightly beyond the heaters. Figure 16 shows an IR image of the evaporator with 275 W applied near the outlet of the evaporator. The flow rate was 79 mL/min. In this case the temperature difference across the entire heat acquisition surface was 40 °C. The cold inlet fluid can be clearly seen at the inlet of the evaporator. The saturation temperature of the fluid was 72 °C. This roughly corresponds to the whitish and red areas on the image (excluding the rectangular heater) which indicates the presence of vapor. While the vapor extends beyond the heaters somewhat, it clearly does not extend over the entire heat acquisition surface. The saturated vapor would need to extend over the entire heat acquisition surface, in order to meet the isothermality requirement.

This lack of isothermality stems from the fact that the liquid and vapor sides of the evaporator have a strong thermal coupling (as discussed above). The evaporator is made of solid aluminum, and relies on a bulky bolted flange to attach the body and the cover plate. This means that the casing contributes to the strong thermal coupling of the liquid and vapor sides. Additionally, internal features of the evaporator also contribute to this coupling. Future designs that thermally decouple the liquid and vapor sides of the evaporator are under development. There is a focus on using alternate designs and alternate (low conductivity) casing materials.

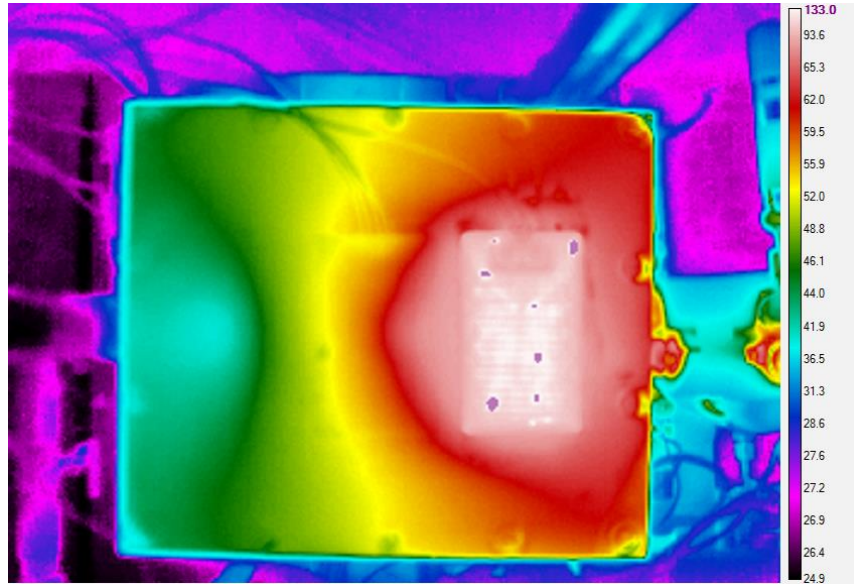


Figure 16. IR image of steady state evaporator showing lack of isothermality. The heater is the white rectangular region. The whitish region beyond the heater is the vapor bubble. The vapor front is unable to advance further in the evaporator cavity because of thermal losses to the cold side of the evaporator.

VI. Conclusion

The Mixed Flow Architecture and Separated Flow Architecture (SFA) were compared experimentally and theoretically in the context of current JPL requirements. These requirements were:

1. Develop a $\sim 1 \text{ m}^2$ planar heat acquisition zone (evaporator) that can:
 - a. Accommodate up to 500 W
 - b. Accommodate heat fluxes up to 5 W/cm^2
 - c. Accommodate distributed discrete heat loads
 - d. Maintain isothermality within a temperature band of $3 \text{ }^\circ\text{C}$ across entire evaporator
 - e. Provide temporal stability of less than $0.05 \text{ }^\circ\text{C/min}$
2. Use less than 5 W of control power
3. Accommodate multiple evaporators and condensers
4. Provide at least a 15 year lifetime
5. Accommodate multiple evaporators and condensers

In the context of these requirements and based on preliminary findings, the SFA architecture is preferable to the MFA architecture on several grounds. Perhaps most importantly, SFA systems are more predictable and amenable to analysis than MFA systems, since they predominately contain separated phases and single phase flow. Additionally, for a given level of performance (power level, isothermality) an SFA system requires less power than an MFA system since no pre-heater is required for nominal operation. Finally, if no pre-heater is used, it appears that producing an isothermal evaporator is more feasible with an SFA system.

An MFA system clearly has the potential to accommodate an evaporator that can meet the thermal requirements outlined above. However the costs associated with such a system are likely higher. Firstly, to achieve a high degree of isothermality will require using a pre-heater to bring the working fluid up to saturation prior to the evaporator. While this required heater power can be offset by using a recuperating heat exchanger between the evaporator inlet and outlet, there will still be a mass and/or power cost. The amount of pre-heat required could be significant if the pump requires a high degree of subcooling (high NPSH). It is anticipated that the flight pump will have a high NPSH, since it will be a centrifugal-type impeller. For the MFA testbed developed at JPL, which used water, the required pre-heat was on the order of 100 W. This likely represents a worst case scenario since water has a high specific heat and the operation point was very far from the critical point, implying that the vapor pressure curve is relatively flat (dP/dT is small). The second significant issue with an MFA system is the lingering threat of two-phase

flow instabilities and the attendant unpredictability of two-phase flow in microgravity¹. This introduces significant uncertainty into the design. A low power system (like the one required here) that does not rely on using large pressure drops or high flow rates to suppress instabilities is especially susceptible to these types of instabilities.

An SFA system circumvents the two major objections brought against MFA systems. Firstly, it greatly reduces the risk of developing two-phase flow instabilities by ensuring that the liquid and vapor phases remain separated throughout the entire system (excepting in the condenser). This separation of phases also makes the system much more amenable to analytic modelling. Secondly, an SFA evaporator has the potential to meet the isothermality requirements described above without the need of a pre-heater. It was experimentally shown that an SFA evaporator was able to produce a small isothermal island at saturated conditions with fluid entering the evaporator 50 °C subcooled.

In order to demonstrate that an SFA system can meet the full programmatic requirements, significant work still needs to be done. Firstly an evaporator that can truly meet the isothermality requirements must be developed. The current evaporator design was completely unable to meet the isothermality requirements. This was likely due to the excessive thermal coupling between the subcooled liquid and the heated surface. Several design approaches are being explored to remedy this including using low-conductivity materials and alternate geometries. The second significant feature that needs to be demonstrated with the SFA system is the implementation of multiple evaporators and condensers. This will be carried out in the next phase of the project.

Acknowledgments

This research was carried out at the Jet Propulsion Laboratory, California Institute of Technology, under a contract with the National Aeronautics and Space Administration. The authors would like to thank Gajanana Birur, Terry Hendricks and Brian Carroll for their technical advice and guidance. The authors gratefully acknowledge the support from the JPL Research and Technology Development office that provided the funding for this work.

© 2017 California Institute of Technology. Government sponsorship acknowledged.

References

- ¹Sunada, Eric, et al. "A Two-Phase Mechanically Pumped Fluid Loop for Thermal Control of Deep Space Science Missions." 46th International Conference on Environmental Systems, 2016.
- ²Ghiaasiaan, S. Mostafa. Two-phase flow, boiling, and condensation: in conventional and miniature systems. Cambridge University Press, 2007.
- ³Ku, Jentung. Operating characteristics of loop heat pipes. No. 1999-01-2007. SAE Technical Paper, 1999.
- ⁴Krotuik – Thermal Hydraulics for Space Power...Ch. 2
- ⁵Park, Chanwoo, Aparna Vallury, and Jon Zuo. "Performance evaluation of a pump-assisted, capillary two-phase cooling loop." *Journal of Thermal Science and Engineering Applications* 1.2 (2009): 022004.
- ⁶Park, Chanwoo, and Michael Crepinsek. "Effect of operational conditions on cooling performance of pump-assisted and capillary-driven two-phase loop." *Journal of Thermophysics and Heat Transfer* 25.4 (2011): 572-580.
- ⁷Furukawa, Masao, and Kazuki Mimura. Development Tests of a Vapor/Liquid Separated Two-Phase Fluid Loop. No. 972477. SAE Technical Paper, 1997.
- ⁸Schweickart, Russell, et al. "Testing of a controller for a hybrid capillary pumped loop thermal control system." *Energy Conversion Engineering Conference, 1989. IECEC-89., Proceedings of the 24th Intersociety. IEEE, 1989.*
- ⁹Delil, A. A. M., A. A. Woering, and B. Verlaat. Development of a Mechanically Pumped Two-Phase CO₂ Cooling Loop for the AMS-2 Tracker Experiment. No. 2002-01-2465. SAE Technical Paper, 2002.
- ¹⁰Bland, T., R. Downing, and D. Rogers. "A two-phase thermal management system for large space platforms." 19th Thermophysics Conference. 1985.
- ¹¹Konishi, Christopher, and Issam Mudawar. "Review of flow boiling and critical heat flux in microgravity." *International Journal of Heat and Mass Transfer* 80 (2015): 469-493.
- ¹²Personnal communication with UTAS.
- ¹³https://www.parker.com/literature/Precision%20Cooling/Two_Phase_Evaporative_Precision_Cooling_Systems.pdf
- ¹⁴<https://www.1-act.com/innovations/pumped-two-phase-cooling/>
- ¹⁵Ku, Jentung, and Edward J. Krolczek. The Hybrid Capillary Pumped Loop. No. 881083. SAE Technical Paper, 1988.
- ¹⁶Sakamoto, Kenichi, et al. "Development of Two-Phase Mechanically Pumped Fluid Loop with Large Isothermal Evaporator using Porous Wick Structure." 47th International Conference on Environmental Systems, 2017.
- ¹⁷Lemmon, Eric W., Marcia L. Huber, and Mark O. McLinden. "NIST reference fluid thermodynamic and transport properties–REFPROP." NIST standard reference database 23 (2002): v9.1